NON-ISOTHERMAL THREE-PHASE FLOW OF PETROLEUM, GAS AND WATER IN T AND Y JUNCTIONS

Wilma Sales Cavalcanti, e-mail: wilmacavalcanti@hotmail.com
UFCG/CCT/UAEM, Bolsista DTI/CNPq

Emanuel Zózimo Gonçalves Belém, e-mail: emanuelbelem@gmail.com
UFCG/CCT/UAEM, Bolsista IC ANP/UFCG-PRH-25

Wagner Celso Paiva Barbosa de Lima, e-mail: gentil_wagner@hotmail.com
UFCG/CCT/UAEM, Bolsista ITI/CNPq

Fabiano Pereira Cavalcante, e-mail: fabiano@jbr.eng.br
JBR Engenharia Ltda

Severino Rodrigues de Farias Neto, e-mail: fariasn@deq.ufcg.edu.br
UFCG/CCT/UAEQ

Antonio Gilson Barbosa de Lima, e-mail: gilson@dem.ufcg.edu.br
Universidade Federal de Campina Grande (UFCG). Unidade Acadêmica de Engenharia Mecânica, Av. Aprígio Veloso, 882, Bodocongó. Caixa Postal: 10069, CEP: 58429-900, Campina Grande, PB, Brasil.

Abstract. *The occurrence of multiphase flow in the petroleum industry is very common in the transport, production and processing facilities of hydrocarbon from oil and gas fields. In the transport facilities, occur multiphase flow when the produced fluids are transferred for other areas through pipelines. In the production systems, the multiphase flow happens, for example, when the fluids inside the reservoirs in deepwater moves until the surfaces through wells, pipelines and risers. Studies about multiphase flow majority are limited to two-phase flows such as: liquid-liquid, liquid-solid, liquid-gas, gas-solid, thus involving only two phase. Few are the research related to three-phases flows specially "T" and "Y" junctions. These junctions when properly used can contribute significantly in the process of phase separation of produce fluids. In this sense, the objective of this work is to study the three-phase flow (water-gas-oil) in T and Y junctions. Simulations were realized using the software CFX-3D. Numerical results of the velocity, pressure, void fraction and temperature distributions of the phases are presented and analyzed.*

Key-words: *Three-phase, modeling, heavy oils, finite volume, junction*

1. INTRODUCTION

In many industrial processes such as fluid flow on offshore oil well platforms, steam injection systems for enhanced recovery of heavy oil, and oil and gas transportation pipeline networks there are two or more phase flowing and it is necessary in some cases, due to safety and economic restrictions to separate or combine the phases for an easier and safer handling.

Traditionally the separation has been carried out by gravity separators, cyclone and hydrocyclone, based in the density differences among the phases. Nevertheless, these efficient equipments require space and weight that it is necessary to avoid, for example, in offshore platforms; as well as to minimize the storage of dangerous substances.

The other side, when two and more phases flows through a junctions, the phases tend to separate in differents proportions (very rarely split in the same ratio) among the outlet arms. The less dense phase, often gas, tends to flow through the side arm (branch), while the denser phase will flow straight through the main arm (run). So an almost inevitable division of the phases occurs between the outlets. Sometimes, for example, all the liquid may by diverted into the branch arm at others times all the liquid may go straight into the run arm (main arm). The liquid volumetric fraction diverted into the branch can be very different from that of the gas depending of the many physical and geometrical parameters of the junction such as inlet and outlet pressure and, length and diameter of the arms. Obviously, to lower pressure greater proportion of fluid passing down that outlet is verified.

The division of the phases in equipment downstream of the junctions can constitute a major problem in operation and control of the process in power industries as well as in oil and gas production (Mak et al., 2006). Besides, in junctions, spatial distribution of the phases is not only effect of interest. In some cases pressure drop is required too.

Due to the importance, more recently, many experimental and theoretical investigations has been reported in the literature about the fluid flow throug junctions, mainly as separators or combinations of phases (Issa and Oliveira, 1994; Penmatcha *et al*., 1996; Roberts *et al*., 1997; Ottens *et a*l., 2001; Moon and No, 2003; Guillot and Colin, 2005; Engl *et al.*, 2006; Hirota *et al.,* 2006; Quian and Lawal, 2006; Stigler, 2007; Tapias, 2007; Xu *et al*., 2008).

Unfortunately, none of these works give a complete understanding of the splitting phenomenon, non are they capable to predict the liquid split very accurately. Besides, all works refers to mono or two phases flows. However, for non- isothermal three-phases, flow in a T and Y-junctions no publications are available. In this sense, the aim of this numerical investigation is to predict thermo-fluid dynamic of the three-phase flow (oil, gas and water) and phase separations through T and Y junctions.

2. MATHEMATICAL MODELING

The mathematical model used to describe the multiphase flow is the model Eulerian-Eulerian inhomogeneous (CFX Solver Theory, 2005). In this case, the governing equations are:

a) Continuity equation

$$\frac{\partial}{\partial t}\left(r_\alpha \rho_\alpha\right)+\nabla \bullet \left(r_\alpha \rho_\alpha \vec{U}_\alpha\right)= S_{MS\alpha}+\sum_{\beta=1}^{N_p}\left(\Gamma_{\alpha\beta}\right) \tag{1}$$

where α and β are the phases involved; r_α is the volume fraction of phase α; ρ_α is the density of phase α; $\vec{U}_\alpha$ is the vector velocity of the phase α; N_p is the number of phases; $S_{MS\alpha}$ describes user specified mass sources, and $\Gamma_{\alpha\beta}$ mass flow rate is mass per unit volume of phase β to phase α. This term only occurs if interphase mass transfer takes place.

b) Momentum Equation

$$\frac{\partial}{\partial t}\left(r_\alpha \rho_\alpha \vec{U}_\alpha\right)+\nabla \bullet \left[r_\alpha\left(\rho_\alpha \vec{U}_\alpha \otimes \vec{U}_\alpha\right)\right]= -r_\alpha \nabla p_\alpha+\nabla \bullet \left\{r_\alpha \mu_\alpha\left[\nabla \vec{U}_\alpha+\left(\nabla \vec{U}_\alpha\right)^T\right]\right\}+$$

$$+\sum_{\beta=1}^{N_p}\left(\Gamma^+_{\alpha\beta}\vec{U}_\beta-\Gamma^+_{\beta\alpha}\vec{U}_\alpha\right)+S_{M_\alpha}+\vec{M}\alpha \tag{2}$$

where μ_α is the dynamic viscosity of phase α ; $S_{M\alpha}$ describes momentum sources due to external body forces, and other user defined momentum sources and M_α describes the interfacial forces acting on the phases α due to the presence of other phases. The term $\left(\Gamma^+_{\alpha\beta}U_\beta-\Gamma^+_{\beta\alpha}U_\alpha\right)$ represents momentum transfer induced by interphase mass transfer.

c) Energy Equation

$$\frac{\partial}{\partial}\left(r_\alpha \rho h_\alpha\right)+\nabla \bullet \left[r_\alpha\left(\rho_\alpha \vec{U}_\alpha h_\alpha-\lambda_\alpha \nabla T_\alpha\right)\right]= \sum_{\rho=1}^{N_p}\left(\Gamma^+_{\alpha\beta}h_{\beta s}-\Gamma^+_{\beta\alpha}h_{\alpha s}\right)+Q_\alpha+S_\alpha \tag{3}$$

where $h_\alpha, \lambda_\alpha, T_\alpha$, denote the static enthalpy, the temperature and thermal conductivity of phase α; S_α describes external heat sources; Q_α denotes interphase heat transfer to phase α across interfaces with other phases. The term $(\Gamma^+_{\alpha\beta}h_{\beta s}-\Gamma^+_{\beta\alpha}h_{\alpha s})$ represents heat transfer induced by interphase mass transfer.

The sum of the void fractions is unitary:

$$\sum_{\alpha=1}^{N_p} r_\alpha = 1 \tag{11}$$

and the same pressure field is used for all the phases as follows:

$$p_\alpha = p_1 = p \qquad 2 \le \alpha \le N_p \tag{12}$$

In order to specify the interphase terms, it is necessary to specify the interfacial area per unit volume and an overall heat transfer coefficient. Interfacial transfer of momentum, heat and mass is directly dependent on the contact surface area between the two phases. This is characterized by the interfacial area per unit volume between phase α and phase β, known as the interfacial area density, $A_{\alpha\beta}$.

The Particle model for interfacial transfer between two phases assumes that one of the phases is continuous (phase α) and the other is dispersed (phase β). The surface area per unit volume is then calculated by assuming that phase β is present as spherical particles of mean diameter d_β. Using this model, the interphase contact area is:

$$A_{\alpha\beta} = \frac{6r_\beta}{d_\beta} \tag{13}$$

Non-dimensional interphase transfer coefficients may be correlated in terms of the particle Reynolds number and the fluid Prandtl number. These are defined using the particle mean diameter, and the continuous phase properties, as follows:

$$\mathrm{Re}_{\alpha\beta} = \frac{\rho_\alpha \left|\vec{U}_\beta - \vec{U}_\alpha\right| d_\beta}{\mu_\alpha} \tag{14}$$

$$\mathrm{Pr}_{\alpha\beta} = \frac{\mu_\partial c_{p_\alpha}}{\lambda_\alpha} \tag{15}$$

where μ_α, c_{p_α} and λ_α are the viscosity, specific heat capacity and thermal conductivity of the continuous phase α.

The following general form is used to model interphase drag force acting on phase α due to phase β.

$$M_\alpha = C_{\alpha\beta}^{(d)}\left(\vec{U}_\beta - \vec{U}_\alpha\right) \tag{16}$$

Note that $c_{\alpha\alpha} = 0$ and $c_{\alpha\beta} = c_{\beta\alpha}$. Hence, the sum over all phases of all interphase transfer terms is zero. The form implemented in ANSYS CFX to describe $C_{\alpha\beta}^{(d)}$ is given by:

$$C_{\alpha\beta}^{(d)} = \frac{C_D}{8} A_{\alpha\beta} \rho_\alpha \left|\vec{U}_\alpha - \overline{U}_\beta\right| \tag{17}$$

where $C_D = 0.44$; ρ is the fluid density, $\overline{U}$ is velocity and A is the projected area of the body in the direction of flow.

Interphase heat transfer occurs due to thermal non-equilibrium across phase interfaces. The total heat transfer per unit volume transferred to phase α due to interaction with other phases is given by:

$$Q_\alpha = \sum_{\beta \neq \alpha} Q_{\alpha\beta} \tag{4}$$

where:

$$Q_{\alpha\beta} = -Q_{\beta\alpha} \quad \Rightarrow \quad \sum_\alpha Q_\alpha = 0 \tag{5}$$

Heat transfer across a phase boundary is usually described in terms of an overall heat transfer coefficient $\vec{h}_{\alpha\beta}$, which is the amount of heat energy crossing a unit area per unit time per unit temperature difference between the phases. Thus, the rate of heat transfer, $Q_{\alpha\beta}$, per unit time across a phase boundary of interfacial area per unit volume $A_{\alpha\beta}$, from phase β to phase α, is given by:

$$Q_{\alpha\beta} = \vec{h}_{\alpha\beta} A_{\alpha\beta}\left(T_\beta - T_\alpha\right) \tag{6}$$

This equation may be written in a form analogous to momentum transfer as follows:

$$Q_{\alpha\beta} = c_{\alpha\beta}^{(h)}\left(T_\beta - T_\alpha\right) \tag{7}$$

where the volumetric heat transfer coefficient, $c_{\alpha\beta}^{(h)}$, is modeled using the correlations described below.

For particle model the volumetric heat transfer coefficient is modeled as:

$$c_{\alpha\beta}^{(h)} = \vec{h}_{\alpha\beta} A_{\alpha\beta} \tag{8}$$

It is often convenient to express the heat transfer coefficient in terms of a dimensionless Nusselt number:

$$\vec{h} = \frac{\lambda Nu}{d} \tag{9}$$

In the particle model, the thermal conductivity λ is taken to be the thermal conductivity of the continuous phase, and the length scale *d* is taken to be the mean diameter of the dispersed phase, as follows;

$$\vec{h}_{\alpha\beta} = \frac{\lambda_\alpha Nu_{\alpha\beta}}{d_\beta} \tag{10}$$

For a particle in a moving incompressible Newtonian fluid, the Nusselt number is a function of the particle Reynolds number *Re* and the surrounding fluid Prandtl number.

It is often convenient to express the heat transfer coefficient in terms of a dimensionless Nusselt number. For a particle in a moving incompressible Newtonian fluid, the Nusselt number is a function of the particle Reynolds number *Re* and the surrounding fluid Prandtl number Pr.

To obtain the heat transfer coefficient we use the RANZ-MARSHALL correlation as follows:

$$Nu = 2 + 0.6\,Re^{0,5}\,Pr^{0,3} \qquad 0 \le Re \le 200 \qquad 0 \le Pr \le 250 \qquad (18)$$

Seeking to simplify the model and the solution of the governing equations, the following considerations were assumed: steady-state flow, laminar flow; three-dimensional flow; incompressible flow; non-isothermic flow; Newtonian fluid; constant term-physical properties; interphase non-drag forces and body force were neglected. The shape of pipe is related to T and Y junctions. Figure 1 illustrates the geometries of the T-junction and Y-junction used in the simulation. Both geometries have 1 inlet and 2 outlet. Table 1 shows the geometric characteristics of the junctions.

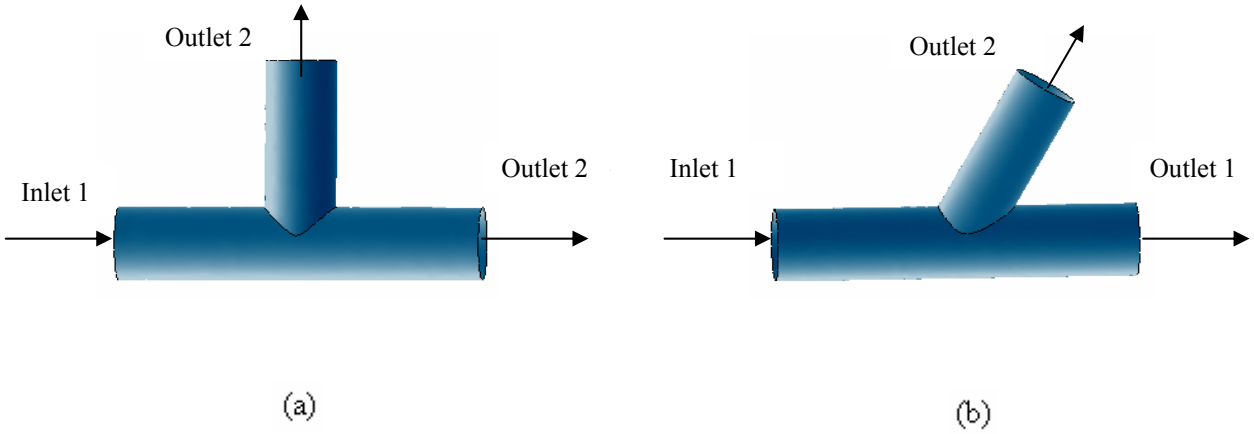

Figure 1. (a)- T-Junction; (b)- Y45º-Junction

Table 1. Geometric characteristics of the junctions

Type of junction	Diameter of main branch (cm)	Diameter of the side branch (cm)	Length of main branch (cm)	Length of side branch (cm)
T	10	9.5	100	50
Y45º	10	9.5	100	50

3. NUMERICAL SOLUTION

The software CFX® was used for generation of the mesh, numerical solution of the governing equations and analysis of the results. CFX® is a commercial simulator for numerical resolution of problems involving fluid mechanics and heat transfer; it uses, the methodology of finite-volumes (Patankar,1980; Versteeg and Malalasekera, 1995; Fortuna, 2002) using non-structured meshes which are more versatile to represents irregular geometries with edges and protrusions .

For the obtaining of the solution of physical problem, we use high-resolution interpolation scheme for the convective terms and Trilinear method for the coupling pressure-velocity. A convergence criterion of 10^{-7} kg/s was used for the mass flow rate. The temperature of the sea water was supposed constant and equal to 25ºC (298 K) in the whole extension of the junction and the fluid temperature in the entrance of the junction was 333K. Properties of the fluids were used according to Table 2.

The following boundary conditions were used:

a) u = v = 0 and w = wo = 0.03m/s in z = 0 for $\forall$ (x,y);

b) u = v = 0 for $\forall$ (x,y,z) / $x^2 + y^2 = R^2$, where R is radius of the junction;

c) In the outlet we consider parabolic conditions and prescribed pressure of 101.325 kPa for all phases.

4 RESULTS AND DISCUSSIONS

4.1 Numerical mesh

This work was developed at the Thermal and Fluids Computational Laboratory, Mechanical Engineering Department, Center of Sciences and Technology, Federal University of Campina Grande. The computer machine used for the simulation was a Pentium4 Dual Core 3.00 GHz , 2048 MB RAM. Figures 2 and 3 show details of the mesh

used, as well as the geometry of the pipe. The T-junction contains 140908 elements and 48025 nodal points and, the Y-junction contains 13562 elements and 47520 nodal points obtained after several grid refinements.

Table 2. Physical properties of the phases used in the simulation

Physical Properties	Value	Source
ρ_a (kg/m^3)	1000	Incropera e DeWitt (2002)
μ_a (N.s/m^2)	1.0 x 10^{-3}	Incropera e DeWitt (2002)
$(c_p)_a$ (J/kgK)	4181.7	Incropera e DeWitt (2002)
k_a (W/mK)	0.6069	Incropera e DeWitt (2002)
ρ_g (kg/m^3)	1.12	Rohsenow et al. (1998)
μ_g (N.s/m^2)	1.78 x 10^{-5}	Rohsenow et al. (1998)
$(c_p)_g$ (J/kgK)	2230	Rohsenow et al. (1998)
k_g (W/mK)	0.03388	Rohsenow et al. (1998)
ρ_o (kg/m^3)	951	Incropera e DeWitt (2002)
μ_o (N.s/m^2)	0.5	Incropera e DeWitt (2002)
$(c_p)_o$ (J/kgK)	1800	Incropera e DeWitt (2002)
k_o (W/mK)	0.147	Incropera e DeWitt (2002)
Surface Tension Coefficient (N m^{-1})	0.08	

4.2 Numerical results

This simulation has the intention to show the behavior of the phases during the flow through the T and Y unctions. It was simulated three-phase flow (oil-water-gas) in the junctions with an inlet and two outlets. In this simulation the elapsed computational time was 6.873 x10^{4}s being accomplished 1000 iterations. The velocity and void fraction of the phases in the inlet of the junctions are specified in Table 3. The oil was taken as continuous phase and water and gas were considered like dispersed phases.

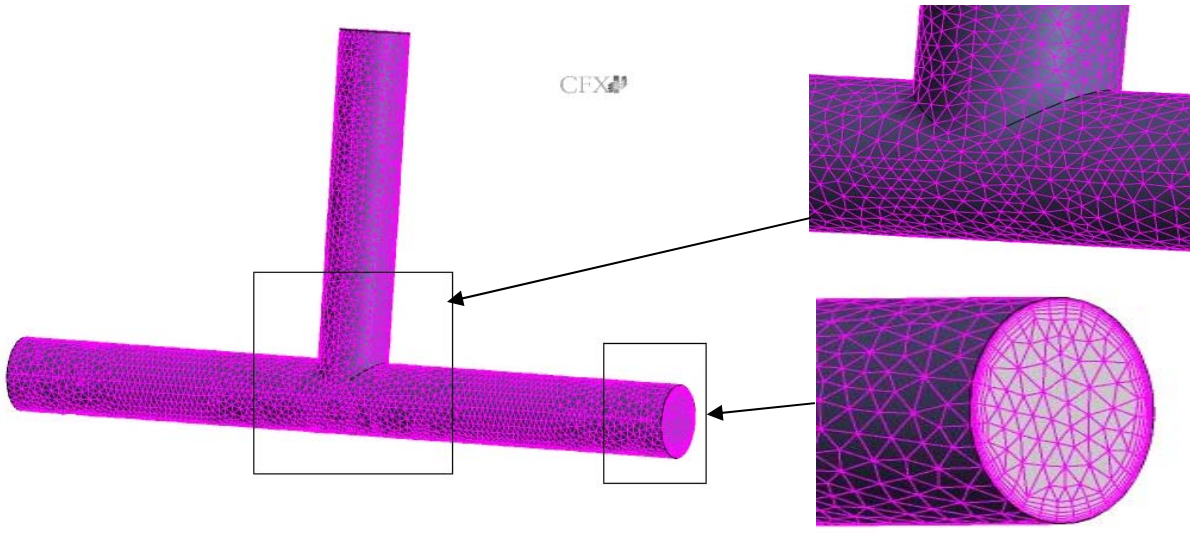

Figure 2. Details of the mesh used in simulations of the T-Junction

Table 3. Characteristics of phases in the inlet of the junctions.

Phases	Velocity (m/s)	Volume fraction	Flux	Particle diameter (mm)
Oil	0.03	0.7	Continuo	----------
Water	0.03	0.2	Dispersed	8
Gas	0.03	0.1	Dispersed	1

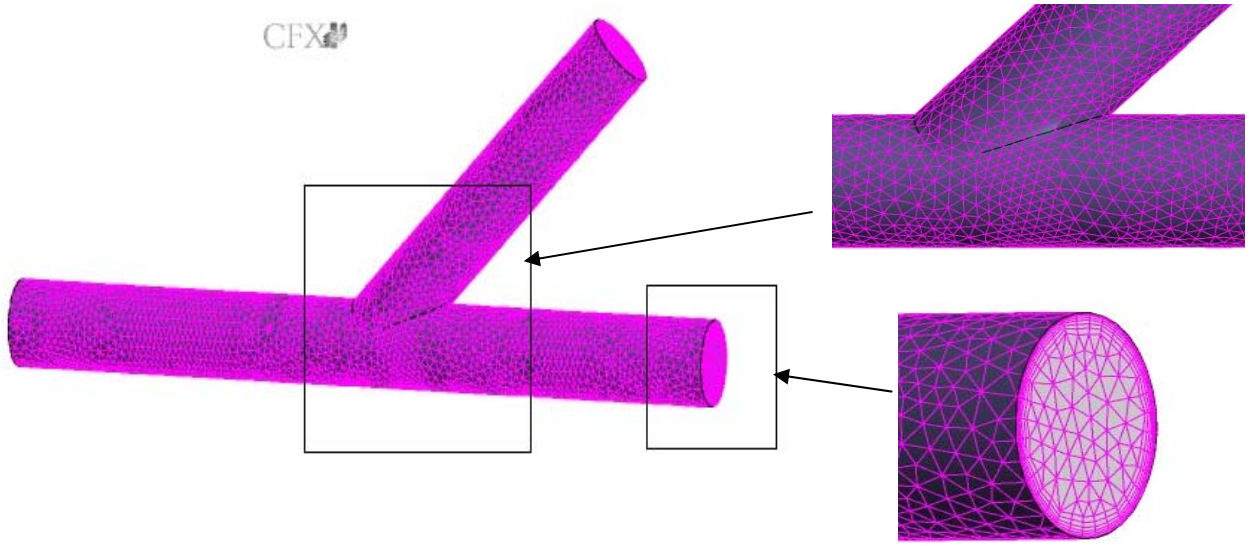

Figure 3. Details of the mesh used in simulations of the Y-Junction

Figure 4 (a) - (b) describes the pressure field of three-phase flow along the junctions (T and Y), in a plan ZX with Y = 0. As expected, the same pressure gradients are observed for all phases and junctions. A decrease of the pressure exists along the flow, with a maximum pressure in the inlet of the pipe and lower pressure in the outlets, as expected. The highest pressure gradients are close to the inlet of the pipe decreasing gradually along the one. A total pressure drop of ΔP=34Pa was necessary to move the mixture gas-oil-water in the whole pipe, without considering the gravity effects (both cases). Few differences were found due to the low velocity of the oil, water and gas phases. Major differences in the pressure field are found when gravity effects are considered in the model.

Figures 5 - 7 illustrates the velocity field of the oil, water and gas phases in the junctions. It can be observed that velocity is zero in the wall and it is going increasing towards the center of the pipe. Due to the no slip condition this effect is transmitted for all layers of fluid adjacent happening the formation of hydrodynamic boundary layer. This increase of the velocity in the center of the junction as occurs fluid flow, it was already waited, because so that there is conservation of the mass, it is necessary an increase of the velocity in the central area of the pipe, to maintain the same mass flow rate. The velocity of the gas and water present highest values as compared to oil velocity, agreeing with the expected.

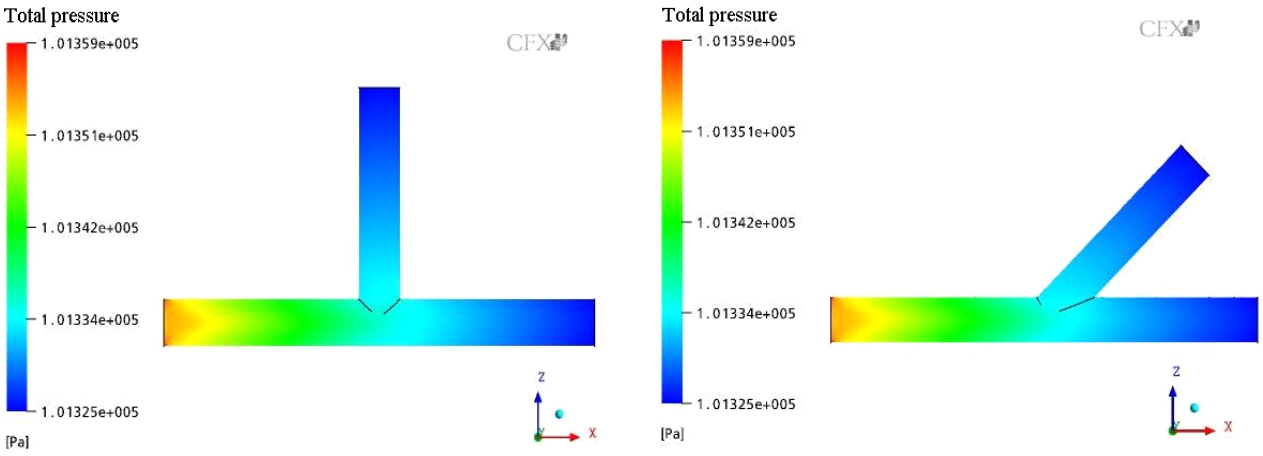

(a) (b)

Figure 4. Pressure distribution in the junctions (a) T and (b) Y45º

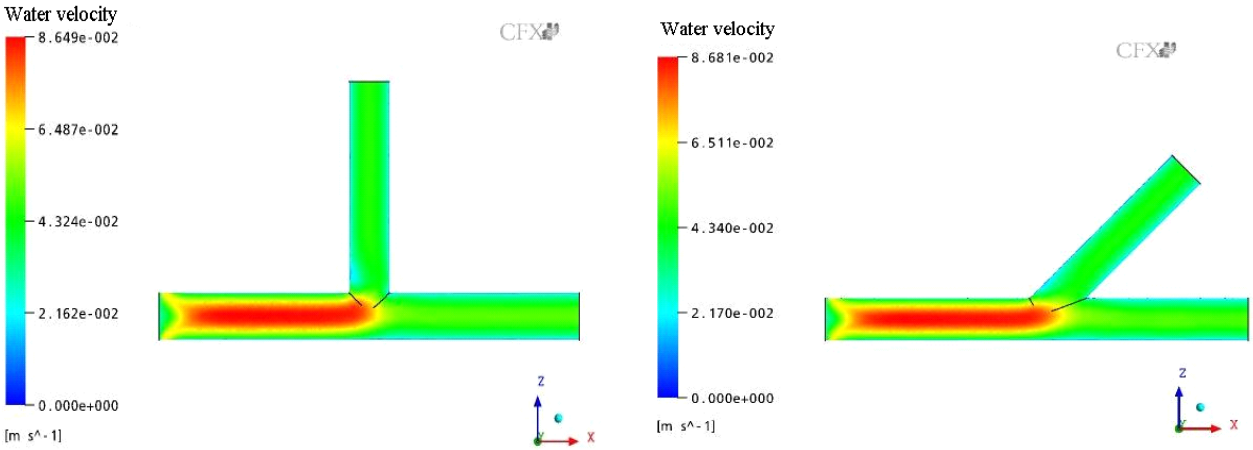

(a) (b)

Figure 5. Water velocity distribution along the junctions (a) T and (b) Y45º.

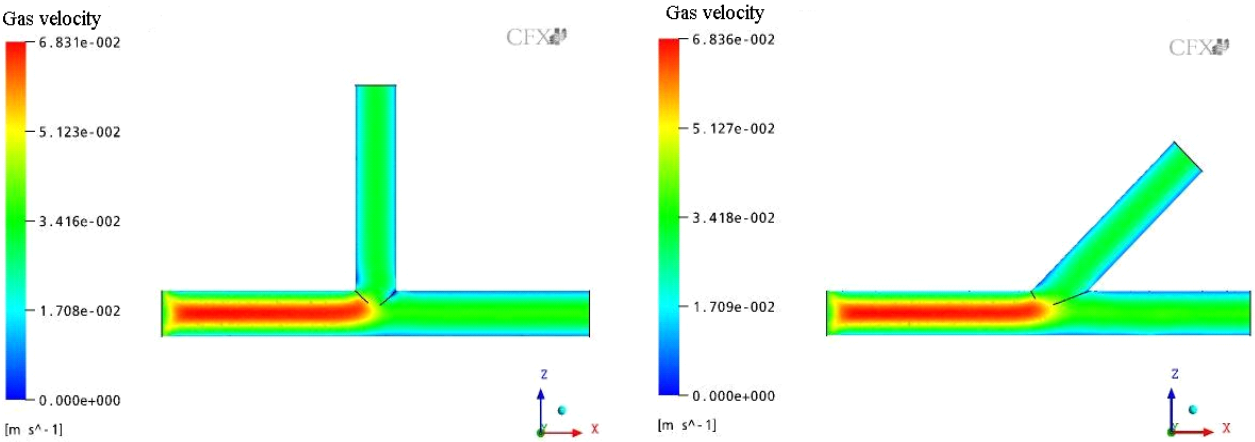

(a) (b)

Figure 6. Gas velocity distribution along the junctions (a) T and (b) Y45º.

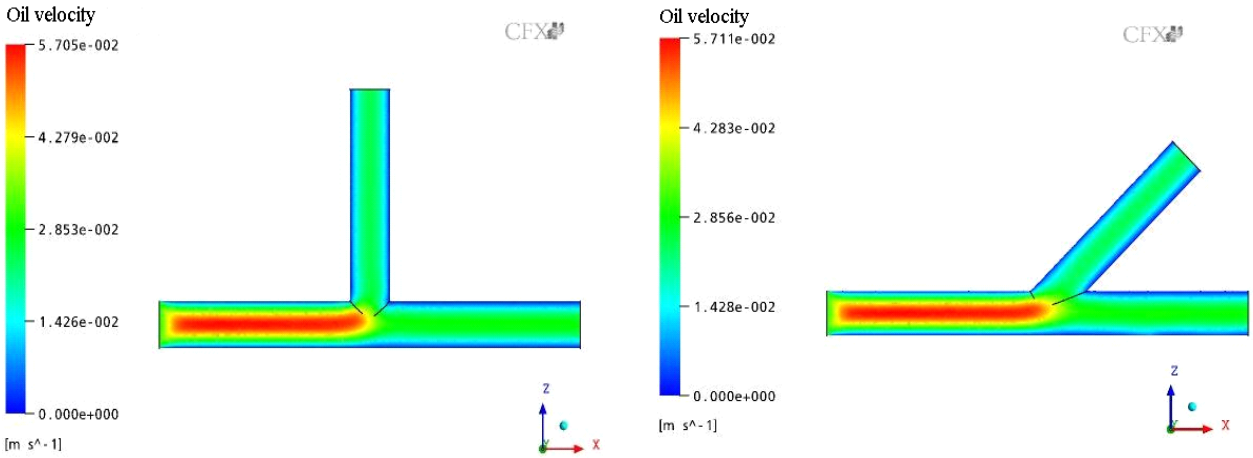

(a) (b)

Figure 7. Oil velocity distribution along the junctions (a) T and (b) Y45º.

Figures 8 - 10 display the void fraction distribution of the oil, water and gas phases. A void fraction 0.1, 0.2 and 0.7 were adopted for the gas, water and oil respectively (the gas phase is dispersed in gas bubbles, water phase is dispersed in drop, and the oils phase exist in continuous form). It can be observed that the oil follows the path preferred by the walls of the duct, while the water is preferably at the center and the gas flow by a path intermediate between the two phases. Stratified flow is verified in the side branch.

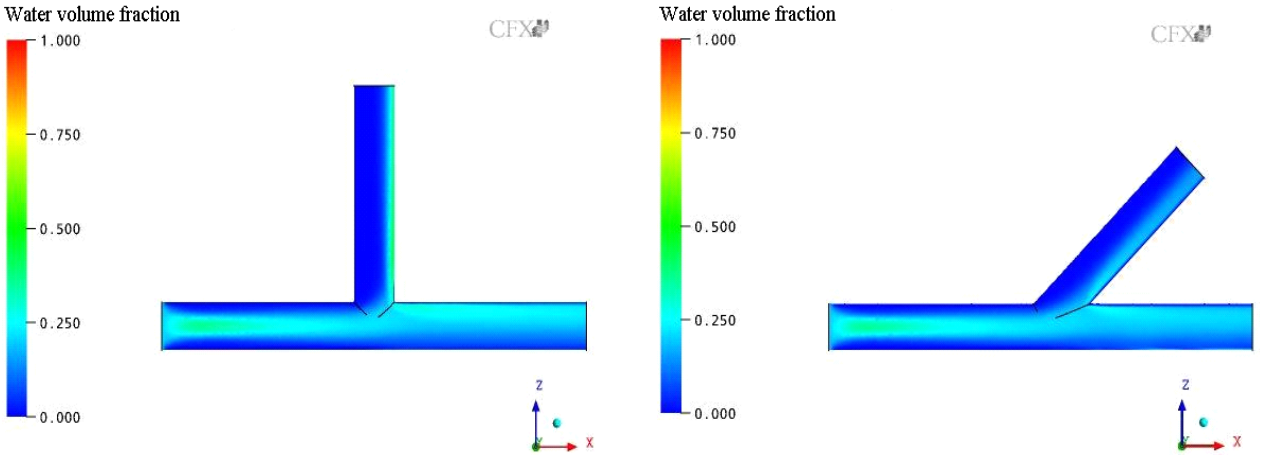

(a) (b)

Figure 8. Volume Fraction of the water in the XZ plane (y=0). (a) T and (b) Y45º.

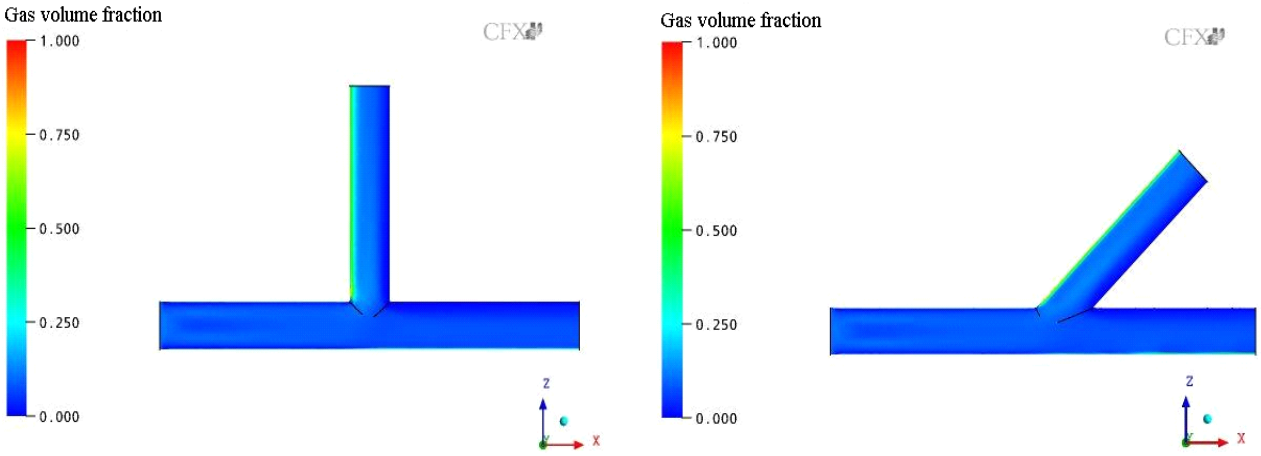

(a) (b)

Figure 9. Volume Fraction of the gas in the XZ plane (y=0). (a) T and (b) Y45º.

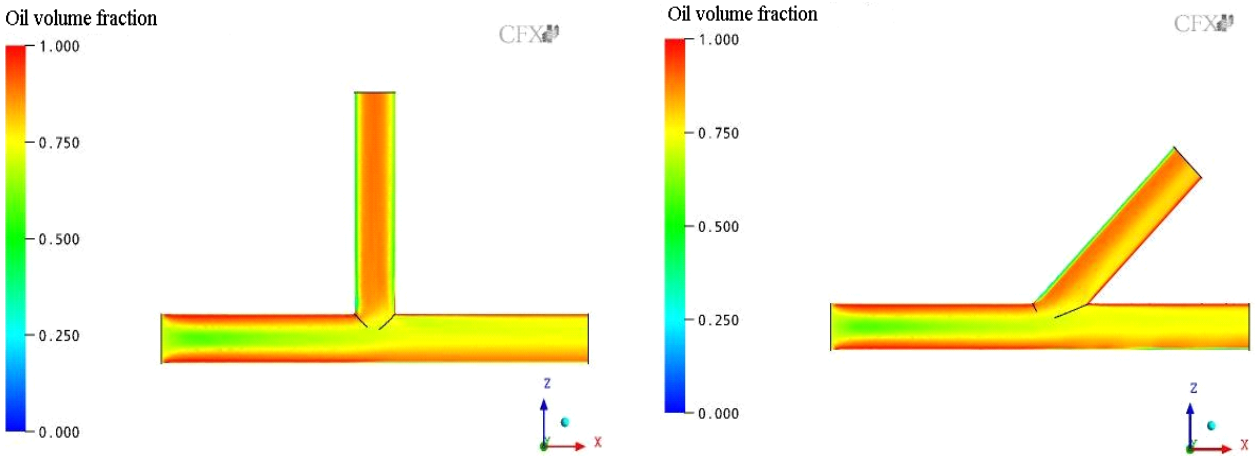

(a) (b)

Figure 10. Volume Fraction of the gas in the XZ plane (y=0). (a) T and (b) Y45º.

Figures 11-13 illustrate the temperature field of the water, gas and oil phases, in T and Y45º-junctions, respectively. It is verified that the wall temperature is 298 K and it rises towards the center of the pipe, where it reaches maximum value. Evidently, due to the heat transfer for the wall of the pipe, the fluid cold along the flow, and appear a thermal boundary layer (Kakaç et al., 1987). Because the higher volume fraction, oil phase it is responsible to heat all fluid flow, so the temperature field of the phases are very similar.

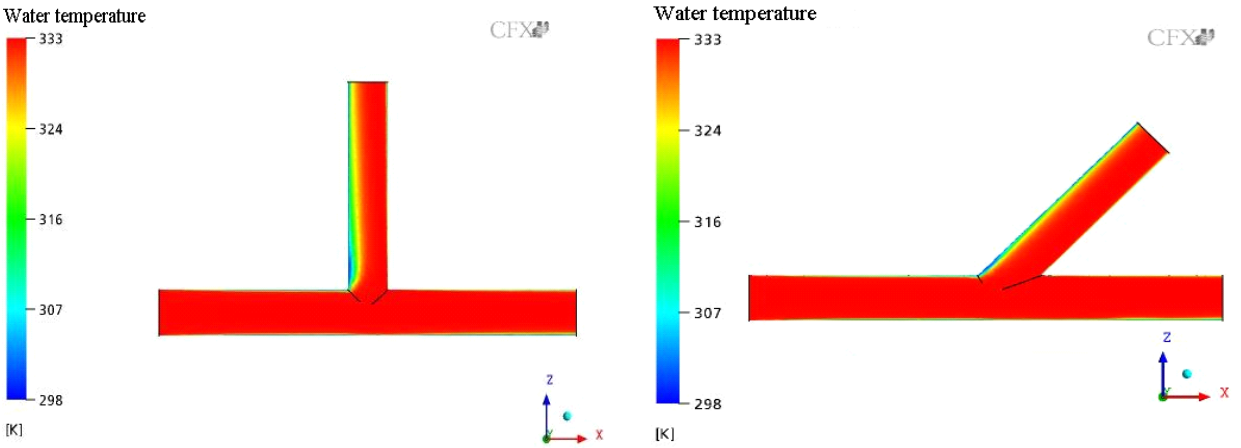

Figure 11. Water temperature distribution in the XZ plane (y=0). (a) T and (b) Y45º.

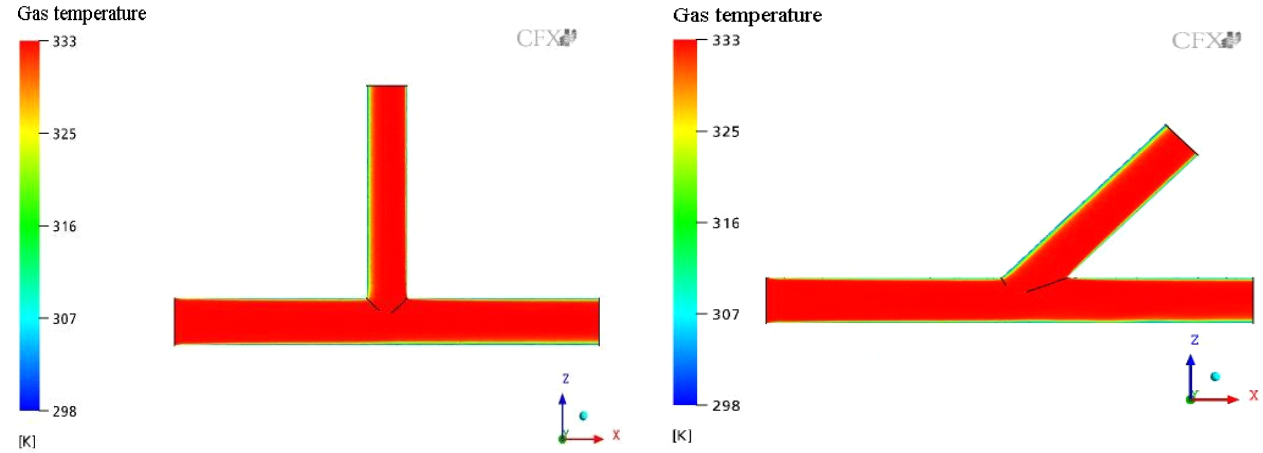

Figure 12. Gas temperature distribution the XZ plane (y=0). (a) T and (b) Y45º.

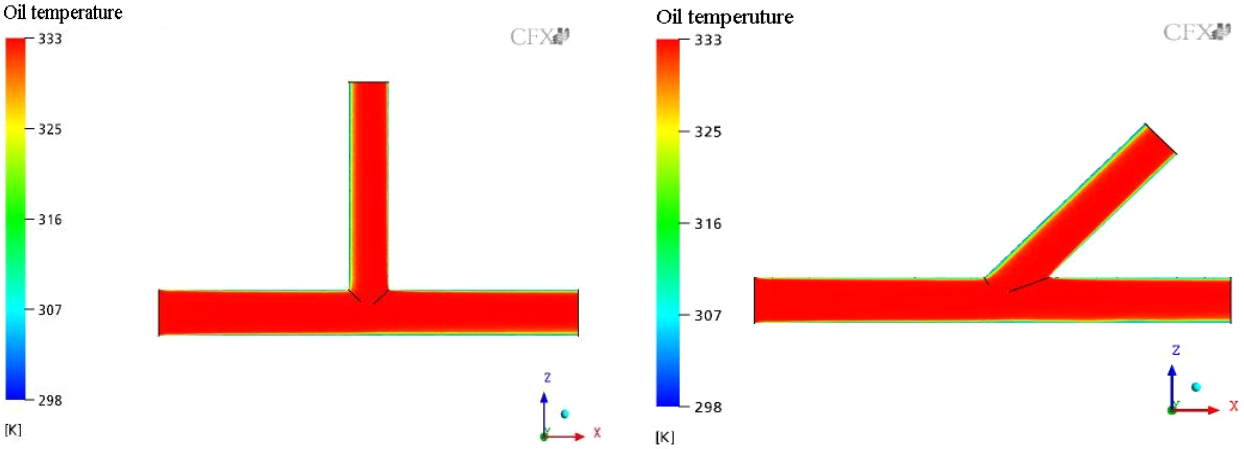

Figure 13. Oil temperature distribution in the XZ plane (y=0). (a) T and (b) Y45º.

Figures 14 - 15 show the temperature profiles in the outlet of the main branch of the junctions for water, gas and oil, respectively. It is observed a very similar behavior. As the volume fraction of oil (70%) is more than gas (10%), the gas that is dispersed in the oil phase, is heated by the oil, so the gas is almost in thermal equilibrium with the oil.

The mass flow rate of each phase at the inlet and outlet of the junction are reported in Table 4. We can see the preferred path for each phase, i.e, the influence of the junction in the separation of phases. Table 5 shows in percentage terms the mass flow rate in the outlet. It is important to note the percentage of each phase in the total flow (gas = 0.1, water= 0.2 and oil= 0.7).

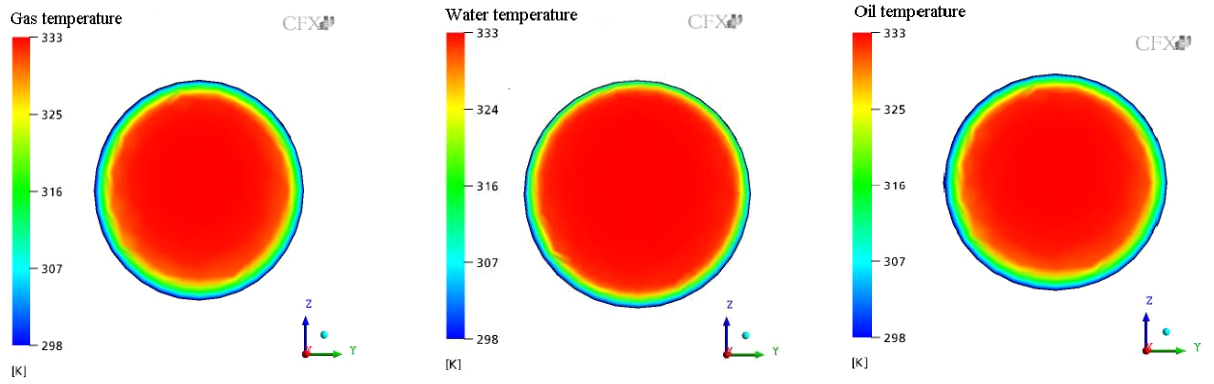

(a) (b) (c)

Figura 14. Temperature distribution in the outlet main branch of the T-junction: (a) oil, (b) water, (c) gas.

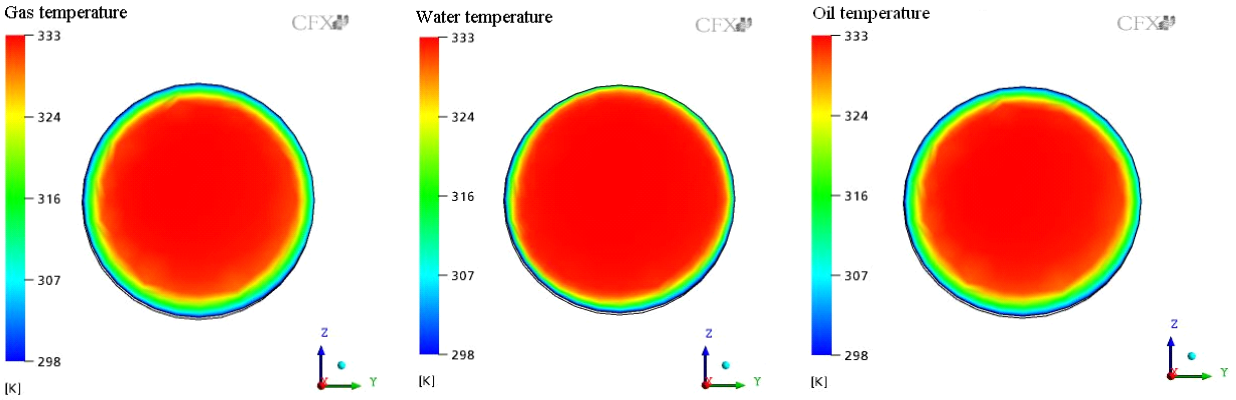

(a) (b) (c)

Figura 15. Temperature distribution in the outlet main branch of the Y45º-junction: (a) oil, (b) water and (c) gas.

Table 4. Mass flow rate of each phase.

	Mass flow rate (kg/s) (T-junction)			Mass flow rate (kg/s) (Y-junction)		
	water	gas	oil	water	gas	oil
inlet	4.6822×10^{-2}	2.6220×10^{-5}	1.5585×10^{-1}	4.6822×10^{-2}	2.6220×10^{-5}	1.5585×10^{-1}
outlet 1	3.6670×10^{-2}	1.1468×10^{-5}	8.2241×10^{-2}	3.4754×10^{-2}	1.2371×10^{-5}	8.6815×10^{-2}
outlet 2	1.0161×10^{-2}	1.4720×10^{-5}	7.3622×10^{-2}	1.1521×10^{-2}	1.3475×10^{-5}	6.9267×10^{-2}

Table 5 shows that the phases with higher density (oil and water) have increased the mass flow rate in the outlet 1 (main branch), while the lower density phase (gas) presents higher mass flow rate in the outlet 2 (side branch). By comparing the effect of separation due to each junction (T and Y45º) it was observed very similar results in accordance with research of Moldonado and Bardalo (2001) applied for two phase flow. Whereas the flow is laminar, i.e., low velocity, and effect of the gravity force was not considered, the main factors that affect the flow are the density and viscosity.

Table 5. Mass flow rate in percentage terms at the outlet of the junction

	Mass flow rate (T-junction)			Mass flow rate (Y-junction)		
	water	gas	oil	water	gas	oil
outlet 1	78.31 %	43.737 %	52.769 %	74.226 %	47.181 %	55.704 %
outlet 2	21.701 %	56.140 %	47.239 %	24.606 %	51.392 %	44.445 %

5 CONCLUSIONS

In concordance with the results obtained, we can conclude in general that:

- The software CFX 10.0 was efficient to describe the three-phase flow, in view of the behavior of the volume fraction, velocity, temperature and pressure profiles in a section of junction.

- It was found that the pressures were identical in outlet of the junctions. It was observed a ΔP of 34 Pa for both T and Y45º-junctions. This pressure was necessary to move the flow across the junction, without to consider the gravity effect.
- The separation efficiency of the phases was greater at the Y-junction It was found that the phases with higher density (oil and water) have increased the mass flow rate in the outlet 1 (main branch) around 74% and 56% respectively, while 52%the lower density phase (gas) moves to outlet 2 (side branch).
- The field of temperature display the formation of thermal boundary layer, showing that the flow is still so far from becoming fully developed.

6. ACKNOWLEDGMENTS

The authors thank to CNPq, ANP/UFCG-PRH-25, FINEP, PETROBRAS, JBR Engenharia Ltda and CT-PETRO, for the granted financial support and to the researchers reported that with their researches, they helped in the improvement of this work.

6. REFERENCES

CFX SOLVER THEORY, 2005, "Manual Ansys CFX 10.0", ANSYS.

Engl, W., Ohata, K., Guillot, P., Colin, A. and Panizza, P., 2006, "Selection of Two-phase Flow Patterns at a Simple Junction in Microfluidic Devices", Physical Review Letters, Vol. 96, pp.134505-1-1345054.

Fortuna, A.O., 2002, "Técnicas Computacionais para Dinâmica dos Fluidos": Conceitos Básicos e Aplicações", Ed. Universitária de São Paulo, Brasil.

Guillot, P. and Colin, A., 2005, "Stability of Parallel Flows in a Microchannel After a T Junction", Physical Review E Vol. 72, No. 6, pp. 066301-1-066301-4

Hirota, M., Asanop, H., Nakayama, H., Asano, T. and Hirayama, S., 2006, "Three-Dimensional Struture of Turbulent Flow in Mixing T-Junction", JSME International Journal, Vol. 49, No. 4, pp. 1070-1077.

Incropera, F.P., DeWitt, D.P., 2002, "Fundamentals of Heat And Mass Transfer", Ed. John Wiley & Sons, New York, 981 p.

Issa, R.I. and Oliveira, P.J., 1994, "Numerical Prediction of Phase Separation in Two-Phase Flow Through T-Junctions", Computers Fluids, Vol. 23, No. 2, pp. 347-372.

Kakaç, S; Shah, R. K.; Aung, W. 1987 "Basics Handbook of single-phase convective heat transfer". John Wiley & Sons, Inc., Canadian.

Mak, C.Y., Omebere-Iyari, N.K., Azzopardi, B.J., 2006 "The split of vertical two-phase flow at a small diameter T-junction", Chemical Engineering Science, Vol. 61, No.19, pp. 6261-6272.

Maliska, C.R., 2004, "Transferência de Calor e Mecânica dos Fluidos Computacional**"**, LTC, Rio de Janeiro, Brasil, 424 p

Moldonato, J.C.S. and Bardalo, S.N., 2001, "Two- Phase Flow Through T-Branch", XVI Brazilian Congress of Mechanical Engineering, CD-ROM, pp.1-7.

Moon, Y.M. and No, H.C., 2003, "Off-Take and Slug Transition at T-Junction af Vertical-up Branch in the Horizontal Pipe", Journal of Nuclear Science and Technology, Vol. 40, No. 5, pp. 317-324.

Ottens. M., Hoefsloot, C.J.H. and Hamersma, J.P., 2001, "Transient Gás-Liquid Flow in Horizontal T-Junctions", Chemical Engineering Science. Vol.56, No. 1, pp. 43-55.

Quian, D. and Lawal, A., 2006, "Numerical Study on Gas and Liquid Slugs for Taylor Flow in a T-Junction Microchannel", Chemical Engineering Science, Vol. 61, No. 23, pp. 7609-7625.

Patankar, S.V., 1980, "Numerical Heat Transfer and Fluid Flow", Ed. Hemisphere Publishing Corporation, New York.

Penmatcha, V.R, Ashton, P.J. and Shoham, O., 1996, "Two-Phase Stratified Flow Splitting at a T-Junction With an Inclined Branch Arm", International Journal of Multiphase Flow, Vol. 22, No. 6, pp. 1105-1122.

Roberts, P.A., Azzopardi, B.J and Hibberd, S., 1997, "The Split of Horizontal Annular Flow at a T-junction", Chemical Engineering Science, Vol. 52, No. 20, pp. 3441-3453.

Rohsenow, W.M. Hartnett J.P. Cho, Y.I., 1998, "Handbook of Heat Transfer", Third Edition, Ed. Mc Graw-Hill.

Stigler, J.,2007, "Mathematical Model of the Unsteady Fluid Flow Through Tee-Junction", Proceeding of the 2nd IAHR International Meeting of the Workgroup on Cavitation and Dynamic Problems in Hydraulic Mechinery and Systems, Timisoara, Romania. pp. 83-92.

Tapias, J.L., 2007, "Pipe Separator and T Junctions", MSc Thesis, Cranfield University, 115 p.

Versteeg, H. K. and Malalasekera, W., 1995, "An Introduction to Computational Fluid Dynamics the Finite Volume Method"; England: Pearson Education Limited.

Xu, J.H., Li, S.W., Tan, J. and Luo, G.S., 2008, "Correlations of Droplet Formation in T-Junction Microfluidic Devices: From Squeezing to Dripping", Microfluidics and Nanofluidics, Vol.5, No.6, pp. 711-717.